

Stabilized porous silicon optical superlattices with controlled surface passivation

M. Ghulinyan,^{1,a)} B. Gelloz,² T. Ohta,² L. Pavese,³ D. J. Lockwood,⁴ and N. Koshida²

¹*Micro-Technology Lab., FBK-irst, via Sommarive 18, Povo I-38050, Trento, Italy*

²*Graduate School of Eng., Tokyo University of Agriculture and Technology, Koganei, Tokyo 184-8588, Japan*

³*Nanoscience Laboratory, Department of Physics, University of Trento, Via Sommarive 14, Povo, I-38050 Trento, Italy*

⁴*National Research Council of Canada, Ottawa, Ontario, K1A 0R6, Canada*

(Received 5 July 2008; accepted 21 July 2008; published online 14 August 2008)

We report on very effective stabilization of porous silicon optical devices through a chemical surface modification technique. Such a chemical treatment proves to alter the growth of native silicon oxide on pore surfaces and thus prevents the optical device from chemical aging. As an example, we apply this technique to one-dimensional freestanding optical superlattices made of five coupled microcavities. We demonstrate how the transmission resonances of the superlattice stabilize after treatment, which implies that refractive indices in the multilayer structure remain constant. The effectiveness of the chemical surface modification technique guarantees a long-life functionality of porous silicon-based optical devices. © 2008 American Institute of Physics. [DOI: 10.1063/1.2969294]

Nanocrystalline porous silicon (PS), produced by electrochemical etching of bulk Si in HF solution, is a material enabling various optoelectronic device applications based on Si.¹ Efficient and stable photoluminescence and electroluminescence have been achieved recently.^{2–4} On the other hand, the relatively cheap and fast production technology of PS offers a rich experimental field to test new ideas. Changing the current (and thus the PS porosity) during etching allows the fabrication of various types of one-dimensional (1D) photonic structures, such as distributed Bragg reflectors, Fabry–Perot optical microcavities and rugate filters.^{5,6} Moreover, 1D passive photonic superlattices^{7,8} have allowed the demonstration of optical analogues of classical electronic phenomena, such as photonic Bloch oscillations, Zener tunneling, and Anderson localization of light waves⁹ and, very recently, a vapor-driven optical switch.¹⁰

In the case of photonic applications, the structural inhomogeneities of PS at the nanoscale appear unresolvable for visible and infrared light, which allows the material to be described by a unique refractive index n within the effective medium approach. This refractive index is lower than that of bulk Si and can be continuously varied over a relatively wide range (~ 1.1 – 3) by varying the porosity and/or oxidation state of the material.⁵

As opposed to these advantages, PS suffers from aging phenomena; the huge internal surface of the pores tends to be progressively oxidized or contaminated by impurities when in contact with air. The oxidation, in particular, leads to a lowering in the effective refractive index with time, which is crucial for a photonic device. In fact, the resonant nature of such devices, where up to hundreds of quarter-wavelength and half-wavelength layers are stuck together, is extremely sensitive to slight changes in n and is detuned easily due to oxidation.⁸ An example is given in Fig. 1 where the reflection spectra of a dielectric mirror structure measured freshly

after anodization and 16 months later are reported. The significant blueshift in the reflection spectra, caused by aging, is clearly observed. Therefore, chemical aging is an issue for PS-based photonic devices and a successful prevention of such a phenomenon is needed.

In this letter we demonstrate very effective stabilization of porous silicon optical devices through a chemical surface modification technique. As a specific example, we show how the spectral response of a freshly prepared optical superlattice is stabilized after a chemical modification of the PS surface when a majority of metastable Si–H bonds are changed into stable Si–C ones.

The optical superlattice was built up by coupling five identical half-wavelength cavities through dielectric Bragg mirrors using two types of $\lambda/4$ -thick dielectric materials A and B . The structure sequence can be presented as Mirror/Cavity₁/Mirror/Cavity₂···/Cavity₅/Mirror, where Mirror= $BABABABAB$ denotes the dielectric mirror, while Cavity _{m} = AA stands for the cavities.^{7,8}

The samples were grown by controlled electrochemical etching of heavily doped ($0.01 \Omega \text{ cm}$) p -type (100)-oriented silicon wafers. The electrolyte was prepared by mixing a 30% volumetric fraction of aqueous HF (48 wt %) with ethanol. A magnetic stirrer was used to improve electrolyte exchange. We applied 50 mA/cm^2 for the high porosity layer A (refractive index $n_A=1.5$) and 7 mA/cm^2 for the low porosity layer B ($n_B=2.1$). The physical thicknesses of the layers were controlled by adjusting the duration of the etch times.

The natural refractive index drifts, which are usually present in relatively thick multilayer PS samples, can be compensated by adjusting the etching times of the layers (see, e.g., Ref. 7 for details). For the studied samples such a tuned optical path ($n \times d$ product) is thus constant to a first order approximation. The superlattice structures were made freestanding by applying an electropolishing current pulse at the end of the growth process.

^{a)}Electronic mail: ghulinyan@fbk.eu.

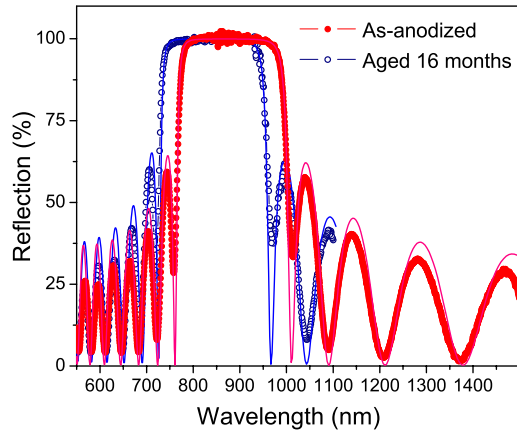


FIG. 1. (Color online) Reflection spectra of a freshly anodized ten-period dielectric mirror (red, \bullet) and after 16 months of storage in air (blue, \circ) are plotted together with the transfer matrix modeling (red and blue solid lines).

Transmission and reflectance spectra of the samples were measured in the wavelength range from 800 to 2200 nm by a Hitachi U-4100 spectrophotometer. In Fig. 2 we show both the experimental transmission spectrum and the theoretical one calculated through a standard transfer matrix formalism.¹¹ Quite good agreement between the spectra indicates the effectiveness of the drift-compensation procedure during the sample growth. In fact, in order to observe the splitting of the cavities degeneracy and the formation of the fine-peaked transmission miniband (as seen in Fig. 2 around 1600 nm), the cavity layers should have almost perfectly tuned $\lambda/2$ optical thicknesses.

To address the aging issue, we firstly quantify the oxidation degree in layers of various porosity. Figure 1 shows the reflection spectra of a dielectric mirror structure measured freshly after anodization and 16 months later, together with the theoretical fits. The structure has been made using a similar silicon substrate and the same etching current densities as for the superlattice samples of Fig. 2. A large, almost 45 nm blueshift of the spectra is measured (Fig. 1, empty circles),

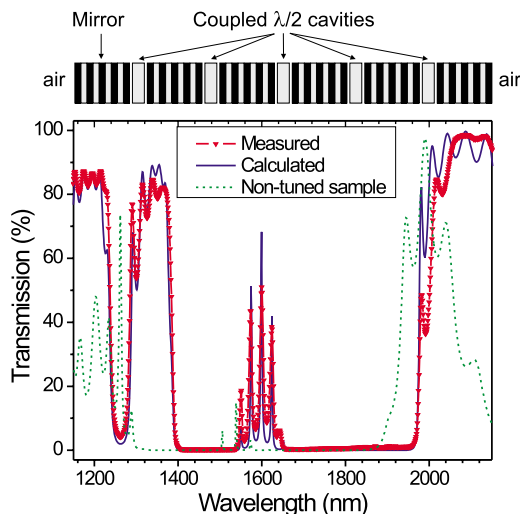


FIG. 2. (Color online) The measured and calculated transmission spectra of the as-anodized PS superlattice constituted of five coupled microcavities. The spectrum of a sample with noncompensated natural drifts is plotted for comparison (dotted line). The multilayer structure is sketched at the top.

which is related to a change of the refractive index caused by the natural oxidation of porous layers.

The calculated theoretical spectrum for the as-anodized sample fits very well the experimental data. From this modeling we extract the physical thicknesses of the various layers to fit the aged sample spectrum. To do this, the refractive indices of the layers have been recalculated using a three-component (i.e., air, silicon, and silicon oxide) effective medium approach. This model considers that some fraction x of Si in the porous silicon skeleton has been oxidized to form SiO_2 which coats the pore surfaces.

Intuitively, the high (A type) and low (B) porosity layers are oxidized differently, because of the different inner surface area of pores. Thus, we introduce two different fractions x_A and x_B . It is possible to calculate that $x_A/x_B \sim (1-p_B)/(1-p_A)$, with p_A and p_B being the porosities of layers A and B , respectively. With these considerations, we found a very good fit to the aged samples spectrum (Fig. 1) and, thus, reliable estimates of $x_A \approx 14.5\%$ and $x_B \approx 6.5\%$.

In order to stabilize the spectral characteristics of the optical superlattices, we have modified the chemistry of the PS surface by a chemical treatment. The derivatization technique is performed as follows: the PS sample was immersed for 3 h in a solution of 1-decene kept at 90 °C. Argon gas was flowed into the solution for about 1 h, before and after the introduction of the sample, to minimize its water content and to eliminate dissolved oxygen in the organic solution. The resulting porous silicon surface stabilization arises from the substitution of metastable silicon-hydrogen bonds by stable silicon-carbon bonds through the covalent attachment of 1-decene.¹²⁻¹⁵

We applied this method to the superlattice of Fig. 2. The freshly treated superlattice transmission spectrum and the zoomed region around the miniband are reported in Figs. 3(a) and 3(b) (dashed lines), respectively. The chemical treatment leads to a slight redshift of the resonances due to a small change in refractive indices induced by the presence of alkyl groups in the PS pores. The transmission spectrum was measured again five months later. Only a minor spectral redshift was observed, contrasting with the large blueshift usually experienced by nontreated superlattices. The measurement performed nine months after treatment did not show any further resonance wavelength shift. Other samples have exhibit similar stability for periods longer than two years. These observations indicate that the chemical surface modification is very effective for PS superlattice stabilization.

It is worth noting that such optical stabilization is extremely important for multilayer structures where refractive index and thickness gradients are present. In fact, when dealing with chemically nontreated PS superlattices, cavity layers with different refractive indices (porosities) and thicknesses will suffer different extents of oxidation. This will lead to a detuning of the compensated optical paths $n \times d$, which in turn will heavily modify the resonant coupling condition.

This is exemplified through transfer matrix calculations as shown in Fig. 3(c). The miniband spectra of the as-anodized (black line) and aged (red line) superlattice sample have been calculated using x_A and x_B values estimated from the fits of dielectric mirrors spectra. Apart from a 50 nm blueshift of the miniband center due to the oxidation, we see how the line shape of the miniband is deformed; the lowered

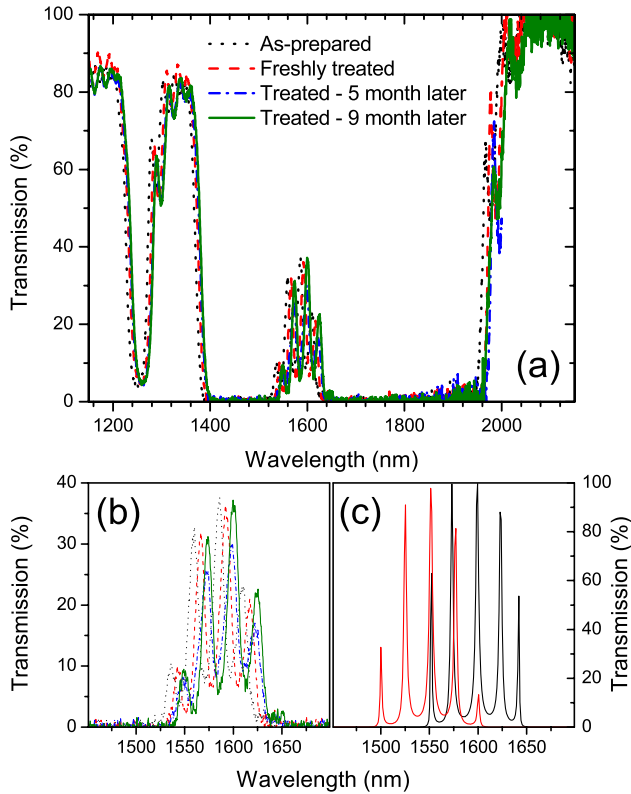


FIG. 3. (Color online) (a) Transmission spectra of the PS superlattice; as-prepared, freshly treated, 5 months after treatment and 9 months after treatment. (b) An expanded view of the transmission miniband region. (c) The calculated transmission minibands for the as-anodized (black line) and aged (red line) optical superlattice, respectively.

index contrast between high and low porosity layers results in a worsening of coupling mirrors and thus less confinement of cavity modes (≈ 10 nm broadening of the original miniband). Moreover, the intensity of the miniband is lowered as well due to less effective coupling between the oxidation-detuned resonant $\lambda/2$ condition of the cavity layers. None of these effects is observed for chemically treated samples [Figs. 3(a) and 3(b)], which strongly evidences the stabilization properties of the surface chemical treatment.

We note that, while the adsorption or condensation of vapors from ambient will still modify the optical properties of such stabilized superlattices, these effects are reversible and can be eliminated by heating slightly the samples or keeping them in a controlled environment. On the contrary, the natural oxidation of as-anodized and not stabilized

samples is an irreversible effect. Therefore, we stress that the chemical stabilization is critically important for a porous photonic device.

In conclusion, we demonstrate the effectiveness of the chemical stabilization method applied to porous silicon-based 1D optical superlattices. The substitution of metastable Si-H bonds by Si-C covalent ones results in a very efficient surface passivation and a chemical protection of porous layers by nano-steric hinderance effects. The effectiveness of the chemical surface modification technique can guarantee a long-life functionality of porous silicon-based optical devices.

The authors wish to thank R. Boukherroub for his suggestions about the chemical modification process. B.G. and N.K. thank the support by a Grant-in-Aid for Scientific Research from MEXT and JSPS in Japan.

¹N. Koshida and N. Matsumoto, *Mater. Res. Soc. Symp. Proc.* **40**, 169 (2003).

²B. Gelloz, A. Kojima, and N. Koshida, *Appl. Phys. Lett.* **87**, 031107 (2005).

³B. Gelloz and N. Koshida, *J. Appl. Phys.* **98**, 123509 (2005).

⁴B. Gelloz, T. Shibata, and N. Koshida, *Appl. Phys. Lett.* **89**, 191103 (2006).

⁵W. Theiß, *Surf. Sci. Rep.* **29**, 95 (1997); M. G. Berger, R. Arens-Fischer, M. Thoenissen, M. Krueger, S. Billat, H. Lueth, S. Hilbrich, W. Theiß, and P. Grosse, *Thin Solid Films* **297**, 237 (1997); L. Pavesi, *Riv. Nuovo Cimento* **20**, 1 (1997).

⁶F. Cunin, T. A. Schmedake, J. R. Link, Y. Li, J. Koh, S. Bhatia, and M. Sailor, *Nat. Mater.* **1**, 39 (2002); E. Lorenzo, C. J. Oton, N. E. Capuj, M. Ghulinyan, D. Navarro-Urrios, Z. Gaburro, and L. Pavesi, *Appl. Opt.* **44**, 5415 (2005).

⁷M. Ghulinyan, C. J. Oton, Z. Gaburro, P. Bettotti, and L. Pavesi, *Appl. Phys. Lett.* **82**, 1550 (2003).

⁸M. Ghulinyan, C. J. Oton, G. Bonetti, Z. Gaburro, and L. Pavesi, *J. Appl. Phys.* **93**, 9724 (2003).

⁹R. Sapienza, P. Costantino, D. S. Wiersma, M. Ghulinyan, C. J. Oton, and L. Pavesi, *Phys. Rev. Lett.* **91**, 263902 (2003); M. Ghulinyan, C. J. Oton, Z. Gaburro, L. Pavesi, C. Toninelli, and D. S. Wiersma, *ibid.* **94**, 127401 (2005); J. Bertolotti, S. Gottardo, D. S. Wiersma, M. Ghulinyan, and L. Pavesi, *ibid.* **94**, 113903 (2005).

¹⁰P. Barthelemy, M. Ghulinyan, Z. Gaburro, C. Toninelli, L. Pavesi, and D. S. Wiersma, *Nat. Photonics* **1**, 172 (2007).

¹¹J. B. Pendry, *Adv. Phys.* **43**, 461 (1994).

¹²R. Boukherroub, S. Morin, D. D. M. Wayner, and D. J. Lockwood, *Phys. Status Solidi A* **182**, 117 (2000).

¹³R. Boukherroub, D. D. M. Wayner, D. J. Lockwood, and L. T. Canham, *J. Electrochem. Soc.* **148**, H91 (2001).

¹⁴R. Boukherroub, D. D. M. Wayner, and D. J. Lockwood, *Appl. Phys. Lett.* **81**, 601 (2002).

¹⁵B. Gelloz, H. Sano, R. Boukherroub, D. D. M. Wayner, D. J. Lockwood, and N. Koshida, *Appl. Phys. Lett.* **83**, 2342 (2003).